# Measurement on Five-Phase
# IM Fed from Ten-Pulse Frequency Converter

Chomát Miroslav, Schreier Luděk, Bendl Jiří

Institute of Thermomechanics AS CR, v.v.i.

*Abstract* — **The mathematical model of a five-phase induction machine derived on base of the theory of space vectors and symmetrical components was verified by means of a comparison of simulation and experimental results. A multi-phase voltage source inverter was used to feed an experimental five-phase induction machine by ten-pulse supply voltage of constant frequency in different connection arrangements. Steady state operation was considered. The good agreement between the simulation and experimental results has proved the correct function of the mathematical and numerical model used.**

*Keywords — Five-phase induction machine, ten-pulse converter, symmetrical components*

## I.  INTRODUCTION

Multi-phase machines have been used in the last few years in electric variable speed drives, for example in ships, electric traction and aircrafts. The application of such machines in some type of drives is given by advantages of the multi-phase machines in comparison with three-phase machines. According to the literature [1] and [2], multi-phase machines have improved magneto-motive force (MMF) waveforms and make it possible to choose a lower voltage for a given output of a machine. Further advantages are the possibility of optimal choice of the control strategy, higher reliability of drives, their increased efficiency and lower noise and especially improved fault tolerance. Nevertheless, it has been remarked that mainly during fault states or unbalance of the feeding system, a necessary behavior analysis of the multi-phase machine must be carried out with regard to the rise of higher spatial harmonics. The analysis of the rise of the spatial harmonics groups and their association with symmetrical components of the instantaneous values of currents and voltages was carried out in [3] for five-phase induction machines and in [4] for six-phase induction machine. This paper presents results of the measurement at an experimental five-phase induction machine fed by a ten-pulse frequency converter in order to verify the results of the theoretical analysis.

## II.  EXPERIMENTAL INDUCTION MACHINE AND FEQUENCY CONVERTER

The five-phase induction machine used for the experimental measurements was built in co-operation with EMP Inc., Slavkov u Brna. The machine was obtained by modification of a standard three-phase two-pole induction machine TM90-2S with the nominal power output of 1.5 kW. The nominal voltage of this machine is 230 $V_{RMS}$, the nominal current 3.2 $A_{RMS}$, and the nominal torque 1.5 Nm. The dimensions and construction arrangement of the five-phase machine including the rotor are the same as for the original machine. Only the number of stator slots was changed from 24 to 30, which enabled substitution of the original three-phase single-layer winding by a five-phase single-layer one. The experimental machine was designed to have the same nominal current as the original machine. For this reason, the shape of the new stator slot was designed so that the sum of all the slot areas, tooth areas and yoke cross section remained the same. The nominal voltage was lowered to 138 $V_{RMS}$. A photo of the experimental machine is in Fig. 1.
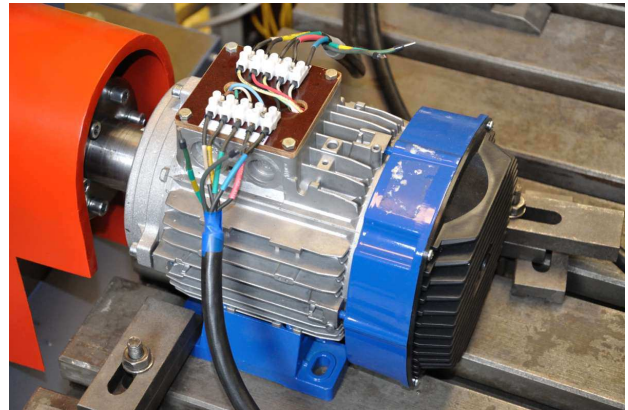


Fig. 1. Experimental five-phase induction motor.

According to [5] and [6], the equations of a five-phase machine derived by means of the theory of space vectors and symmetrical components are

$$u_{1S\alpha} = R_S i_{1S\alpha} + L_{1S}\frac{di_{1S\alpha}}{dt} + L_{1h}\frac{di_{1R\lambda S\alpha}}{dt} \qquad (1)$$

$$u_{1S\beta} = R_S i_{1S\beta} + L_{1S}\frac{di_{1S\beta}}{dt} + L_{1h}\frac{di_{1R\lambda S\beta}}{dt} \qquad (2)$$

$$0 = R_{1RS}i_{1R\lambda S\alpha} + L_{1RS}\frac{di_{1R\lambda S\alpha}}{dt} + L_{1h}\frac{di_{1S\alpha}}{dt} + p\omega_m\left(L_{1RS}i_{1R\lambda S\beta} + L_{1h}i_{1S\beta}\right) \qquad 3)$$

$$0 = R_{1RS}i_{1R\lambda S\beta} + L_{1RS}\frac{di_{1R\lambda S\beta}}{dt} + L_{1h}\frac{di_{1S\beta}}{dt} - p\omega_m\left(L_{1RS}i_{1R\lambda S\alpha} + L_{1h}i_{1S\alpha}\right) \qquad (4)$$

$$u_{3S\alpha} = R_S i_{3S\alpha} + L_{1S}\frac{di_{3S\alpha}}{dt} + L_{1h}\frac{di_{3R\lambda S\alpha}}{dt} \qquad (5)$$

$$u_{3S\beta} = R_S i_{3S\beta} + L_{1S}\frac{di_{3S\beta}}{dt} + L_{1h}\frac{di_{3R\lambda S\beta}}{dt} \qquad (6)$$

$$0 = R_{3RS}i_{3R\lambda S\alpha} + L_{3RS}\frac{di_{3R\lambda S\alpha}}{dt} + L_{3h}\frac{di_{3S\alpha}}{dt} + 3p\omega_m\left(L_{3RS}i_{3R\lambda S\beta} + L_{3h}i_{3S\beta}\right) \qquad (7)$$

$$0 = R_{3RS}i_{3R\lambda S\beta} + L_{3RS}\frac{di_{3R\lambda S\beta}}{dt} + L_{3h}\frac{di_{3S\beta}}{dt} - 3p\omega_m\left(L_{3RS}i_{3R\lambda S\alpha} + L_{3h}i_{3S\alpha}\right) \qquad (8)$$

$$u_{5S} = R_S i_{5S} + L_{5S}\frac{di_{5S}}{dt} + L_{5h}\frac{di_{5R\lambda S\alpha}}{dt} \qquad (9)$$

$$0 = R_{5RS}i_{5R\lambda S\alpha} + L_{5RS}\frac{di_{5R\lambda S\alpha}}{dt} + L_{5h}\frac{di_{5S}}{dt} + 5p\omega_m L_{5RS}i_{5R\lambda S\beta} \qquad (10)$$

$$0 = R_{5RS}i_{5R\lambda S\beta} + L_{5RS}\frac{di_{5R\lambda S\beta}}{dt} + L_{5h}\frac{di_{5S}}{dt} - 5p\omega_m\left(L_{5RS}i_{5R\lambda S\alpha} + L_{5h}i_{5S}\right) \qquad (11)$$

In these equations, the used symbols are commonly used in literature. Further, the subscripts $\alpha$ and $\beta$ represent the real and imaginary parts of the particular symmetrical components of voltages and currents, subscripts 1, 3, and 5 denote the first, the third, and the fifth symmetrical components. The stator quantities are marked by the subscript S. The rotor parameters and current components are rated to the effective number of stator conductors (subscript RS) and rotor current components are converted into the stator coordinate system (subscript $\lambda$). The equations were derived on base of the simplifying assumptions commonly used in the theory of electric machines. In [7], the association between the symmetrical components of currents and individual groups of spatial harmonics of current layer, the magnetic force density along the air gap, and the yoke flux is described. Only the fundamental waves of these groups, i.e., the first spatial harmonic in the case of the first component, the third spatial harmonic in the case of the third component, and the fifth spatial harmonic in the case of the fifth component, have been taken into consideration in derivation of Eqs. (1) to (11). Based on the presented equations, a numerical model of a five-phase induction machine has been developed.

In order to carry out the experiments, the five-phase induction machine was fed from an experimental six-phase voltage-source inverter built in the laboratory, where only five phases were used to generate the output voltages. The photo of the experimental inverter is shown in Fig. 2a.

The power part of the inverter consists of two three-phase IGBT bridges. The electrical power to the DC bus is supplied by a laboratory 6 kW DC voltage source with an adjustable output and additionally smoothed by a bank of DC-link capacitors with the overall capacity of 1000 µF.
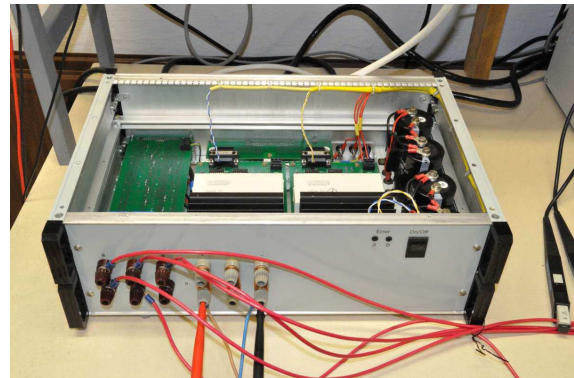


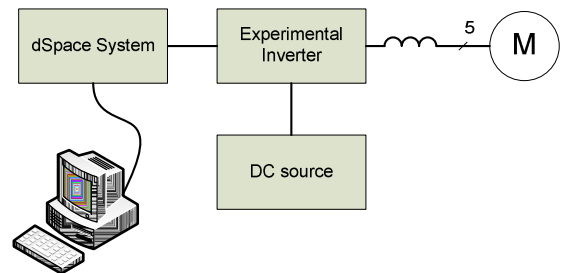Fig. 2a. Experimental six-phase inverter.



Fig. 2b. Schema of experimental setup.

The modulation strategy is realized in the modular dSpace system producing logical inputs for two driver modules. Between the inverter and the motor, filter inductors with induction of 1 mH are connected. A

simplified block schema of the experimental system is shown in Fig. 2b.

### III. SIMULATION AND MEASUREMENT

In the case of feeding a five-phase induction machine from a ten-pulse frequency converter, the third and fifth symmetrical components of voltages arise along with the first one. Therefore, simulation of operation of the machine using the numerical model and comparison of simulation with the experimental results can be used for a verification of the above presented equations. Feeding of a five-phase induction machine from a voltage-source frequency converter of 180-degree valve arrangement is outlined in Fig. 3.
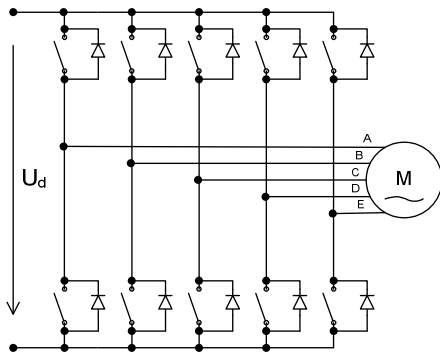


Fig. 3. System under investigation

According to Fig. 4, there are three ways of connecting the stator winding to the converter. The connection according to Fig. 4a will be further denoted as λ, connection according to Fig. 4b as $\delta_1$ and connection according to Fig. 4c as $\delta_2$.

The parameters of the experimental machine were not available during the measurement. Therefore, a machine with main parameters $U_S = 186$ V$_{RMS}$, $R_S = 0.396$ Ω, $R_{1RS} = 0.264$ Ω, $L_{1\sigma S} = 0.0034$ H, $L_{1\sigma RS} = 0.0035$ H, $L_{1h} = 0.0863$ H, $\kappa_{1S} = 0.975$, $\kappa_{3S} = 0.794$ and $\kappa_{5S} = 0.5$ was taken into consideration. The nominal stator phase current is 15.5 A$_{RMS}$ and the nominal power is 7.5 kW. The values of parameters $L_{3h}$, $R_{3RS}$, $L_{3\sigma RS}$, $L_{5h}$, $R_{5RS}$ and $L_{5\sigma RS}$ can be determined by the way described in [6].
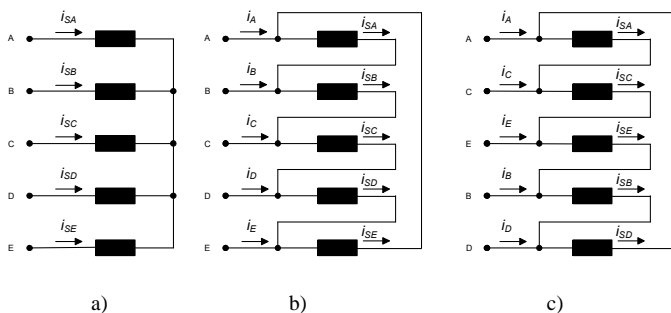


Fig. 4. Connections λ, $\delta_1$ and $\delta_2$ of stator winding to the converter.

The voltages across stator phase A are shown in Fig. 5. The first plot shows the voltage waveform for the case of λ connected stator, the second plot is for the case of $\delta_1$ connection, and the third plot for the $\delta_2$ connection. The

value of the voltage $U_d$ was in all the cases set so that the amplitude of the first time harmonic of the voltage in Fig. 5 was equal to the nominal value of the sinusoidal voltage supply. The voltages of the remaining phases have identical shape and their phase shift is 72°. The waveforms of the real and imaginary parts $u_{1S\alpha}$ and $u_{1S\beta}$ of the first stator voltage symmetrical component, the waveforms of real and imaginary parts $u_{3S\alpha}$ and $u_{3S\beta}$ of the third stator voltage component, and the waveforms of the fifth component $u_{5S}$ are shown in Fig. 6.
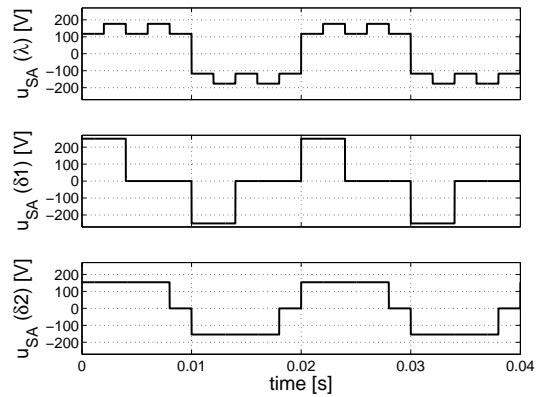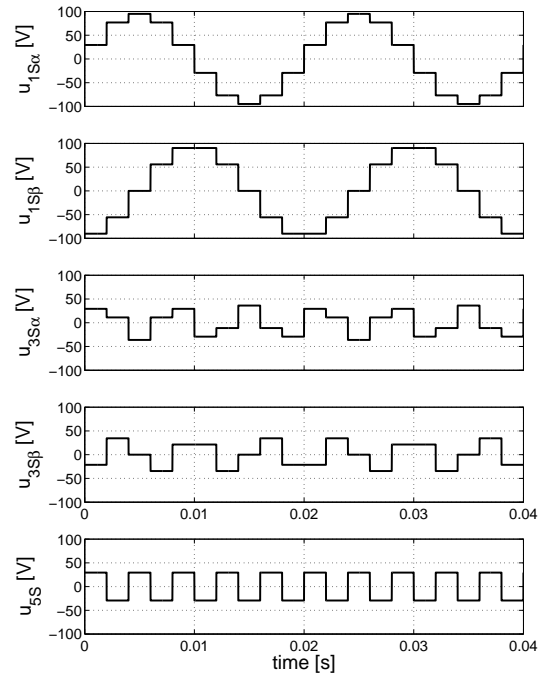


Fig. 5. Phase voltages across phase A.



Fig. 6. Symmetrical components of the stator voltages for λ connection.

As it follows from Fig. 6, the fundamental frequency of the quantities $u_{1S\alpha}$ and $\mu_{1S\beta}$ is 50 Hz and the fundamental frequency of $u_{3S\alpha}$ and $u_{3S\beta}$ is 150 Hz thus frequency of rotation of the third voltage component is triple the frequency of the stator voltage fundamental harmonic.
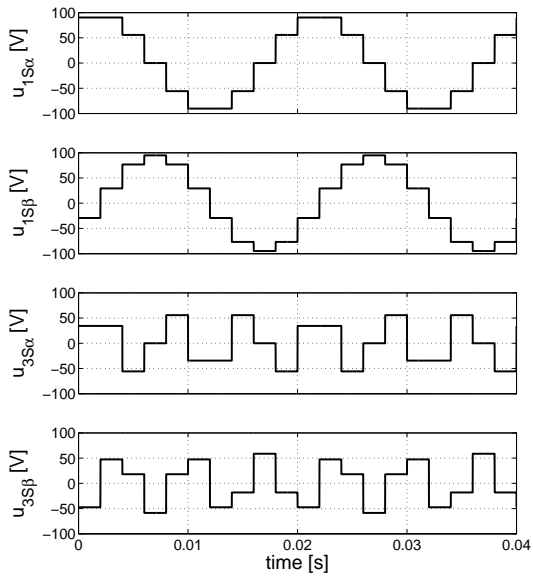
Fig. 7. Symmetrical components of stator voltages for $\delta_1$ connection
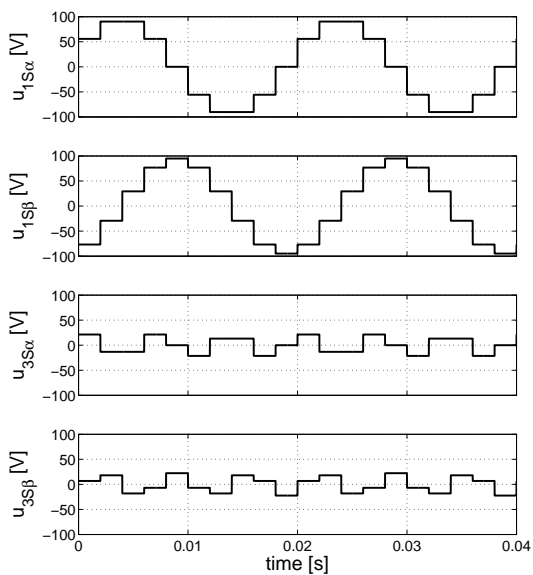


Fig. 8. Symmetrical components of the stator voltages for $\delta_2$ connection

The fifth component is a real quantity, see [5]. In the case of $\lambda$ connection with the insulated node of a stator winding, the current component corresponding to the fifth symmetrical component cannot arise and, therefore, it is not necessary to take the fifth voltage component into consideration.

The waweform of the same quantities as in Fig. 6, but for connections $\delta_1$ and $\delta_2$ are shown in Figs. 7 and 8. The fifth component cannot arise in this case.

Due to the above mentioned way of choosing the value of the voltage $U_d$, the real and imaginary parts of the symmetrical component have the same shape and magnitude. The magnitudes of the real and imaginary components of the third component differ significantly in individual cases. The negative effect of the third spatial

harmonic on machine operation will be minimal in the case of $\delta_2$ and maximal in the case of $\delta_1$. The waveforms of the real and imaginary components of the first and third symmetrical components are shown in Fig. 9 for the case of $\lambda$, in Fig. 10 for the case of $\delta_1$, and in Fig. 11 for the case of $\delta_2$. The waveforms of the current components were simulated for the slip of 0.333 %.
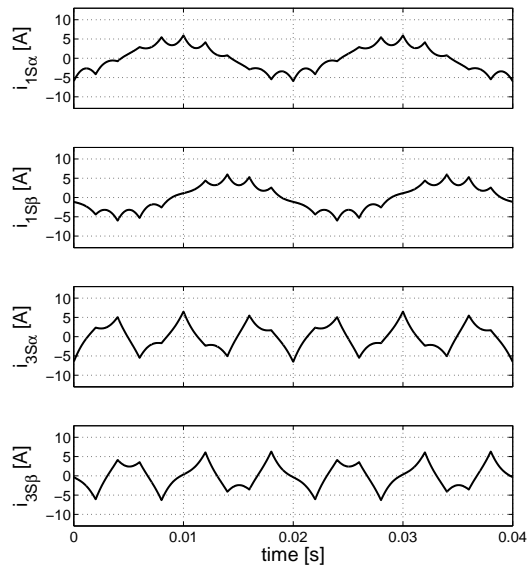


Fig. 9. Symmetrical components of the stator currents for $\lambda$ connection.
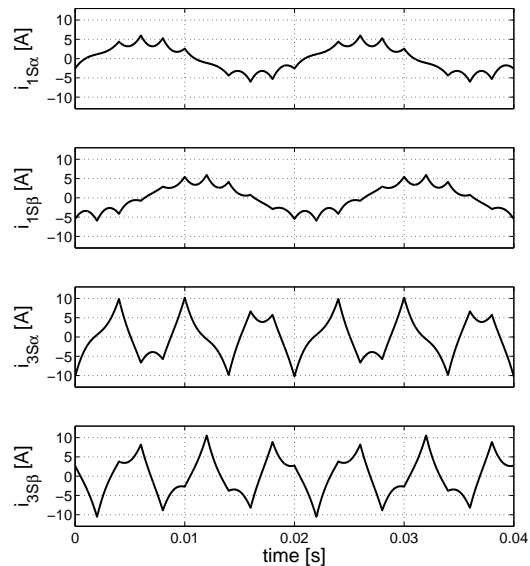


Fig. 10. Symmetrical components of the stator currents for $\delta_1$ connection.

The waveforms of the real and imaginary parts of the first component are similar to each other, while the magnitude of the third component if significantly affected by the magnitudes of the third voltage components. The effect of the third symmetrical component on the

stator currents and converter currents is noticeable from Fig. 12.

The first graph in this figure shows the current $i_{SA}$ in phase A for the $\lambda$ connection. According to [5], the current $i_{SA}$ is twice the sum of $i_{1S\alpha}$ and $i_{3S\alpha}$. The waveforms of the stator current $i_{SA}$ (solid line) and current $i_A$ flowing from the converter (dotted line) are shown in the second plot for $\delta_1$ connection and the currents $i_{SA}$ and $i_A$ are shown for $\delta_2$ connection in the third plot.
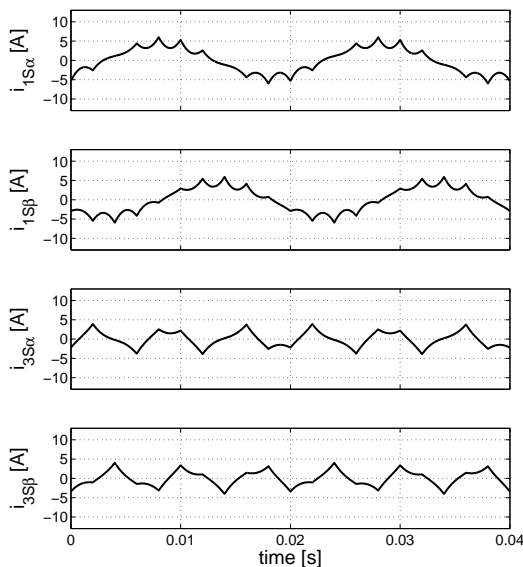


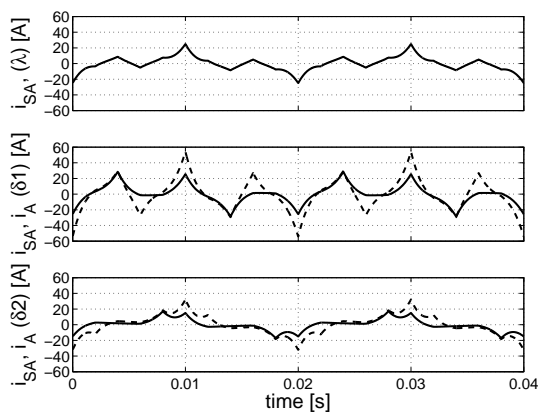Fig. 11. Symmetrical components of the stator currents for $\delta_2$ connection.



Fig. 12. Simulated currents.

The measured waveforms of the currents $i_{SA}$ and $i_A$ for all the considered connections are shown in Fig. 13.

Even though the measurements were made on a machine with different parameters from the ones considered in simulation, the agreement of measurement and simulation is very good as far as the shape of the waveforms is considered.

## IV.  CONCLUSION

Results of the above introduced simulations, considering minimization of the third space harmonic impact on currents in the machine, prove that the $\delta_2$ connection is the most suitable one. In this case, the lowest pulsation torque arises. Another advantage of $\delta_2$-connected stator is a chance to effect magnitude of the voltage in the DC bus. Its minimum value is lower than in the case of $\lambda$ and $\delta_1$ connections. On the contrary, the worst properties from the point of view of the current distortion and magnitudes of pulsation torques are found in $\delta_2$ connection.

The results of the measurement fully verified the validity of the derived equations of a five-phase induction machine and use of the method of space vectors for analysis of a five-phase machine. It is evident that this method can be used for analysis of electric machines with an arbitrary number of phases.

## V.   REFERENCES

[1] Levi, E.: *Multiphase electrical machine for variable-speed applications*, IEEE Transactions on Industrial Electronics, vol. 55, no. 5, 2008, pp. 1893-1909.

[2] Toliyat, H. A.:*Analysis and simulation of five-phase variable-speed induction motor drives under asymmetrical connections*, IEEE Transactions on Industrial Electronics, vol. 15, no. 4, 1998, pp. 748-756.

[3] Schreier, L., Bendl, J., Chomat, M.: *Third Space Harmonics in Five-Phase Induction Machine*, Proc. International Symposium on Electric Machinery, Prague, Czech Republic, 2009, on CD ROM.

[4] Schreier, L., Bendl, J., Chomat, M.: *Influence of space harmonics on properties of six-phase induction machine Part I- Analysis*, Proc. International Conference. on Electrical Machines, (ICEM), Roma, Italy, 2010, on CD ROM.

[5] Schreier, L., Bendl, J., Chomat, M.: *Analysis of five-phase induction machine*," Proc. 15th International Conference on Electrical Drives and Power Electronic. (EDPE), Croatia, 2009, on CD ROM.

[6] Schreier, L., Bendl, J., Chomat, M., Skalka, M.: *Influence of Spatial Harmonics on Properties of Five-Phase Induction Machines*, Proc. 15th International Conference on Electrical Drives and Power Electronic. (EDPE), Croatia, 2009, on CD ROM.

[7] Štěpina, J.: *Fundamental equations of the space vector analysis of electrical machines*, Acta Technica CSAV, no. 2, 1968, pp. 184-198.

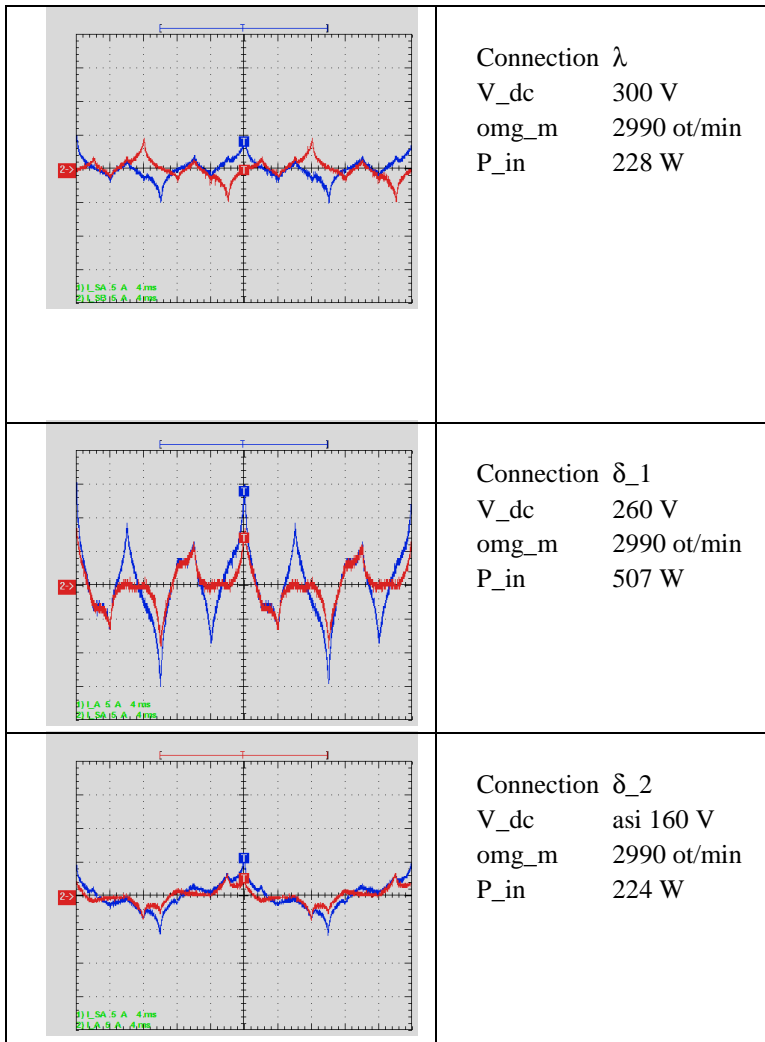| | |
|---|---|
|  | Connection λ<br>V_dc          300 V<br>omg_m      2990 ot/min<br>P_in           228 W |
|  | Connection δ_1<br>V_dc          260 V<br>omg_m      2990 ot/min<br>P_in           507 W |
|  | Connection δ_2<br>V_dc          asi 160 V<br>omg_m      2990 ot/min<br>P_in           224 W |

Fig. 13. Measured currents.

The contribution was presented on the conference ISEM 2011, PRAGUE, CZECH REPUBLIC